

Hybrid Instruments Network Optimization for Air Quality Monitoring

Nishant Ajnoti¹, Hemant Gehlot¹, Sachchida Nand Tripathi^{1,2}

¹Department of Civil Engineering, Indian Institute of Technology Kanpur, India

5 ²[Department of Sustainable Energy Engineering, Indian Institute of Technology Kanpur, India](#)

Correspondence to: Hemant Gehlot (hemantg@iitk.ac.in)

Abstract The significance of air quality monitoring for analyzing the impact on public health is growing worldwide. A crucial part of smart city development includes deployment of suitable air pollution sensors at critical locations. Note that there are various air quality measurement instruments ranging from expensive reference stations that provide accurate data to low-cost sensors that provide **less accurate** air quality measurements. In this research, we use a combination of sensors and monitors, which we call hybrid instruments and focus on optimal placement of such instruments across a region. The objective of the problem is to maximize a satisfaction function that quantifies the weighted closeness of different regions to the places where such hybrid instruments are placed (here weights for different regions are quantified in terms of the relative population density and relative PM_{2.5} concentration). Note that there can be several constraints such as those on budget, minimum number of reference stations to be placed, set of important regions where at least one sensor should be placed and so on. We develop two algorithms to solve this problem. The first one is a genetic algorithm that is a metaheuristic and works on the principles of evolution. The second one is a greedy algorithm that **selects the locally best choice** in each iteration. We test these algorithms on different regions from India with varying sizes and other characteristics such as population distribution, PM_{2.5} emissions, budget available, etc. The insights obtained from this paper can be used to quantitatively place reference stations and sensors in large cities rather than using ad hoc procedures or rules of thumb.

1 Introduction

According to the World Health Organization (WHO), ambient air pollution is a significant threat to people's health, causing around 6.7 million premature deaths annually in 2019 (Fuller et al., 2022). Shockingly, 99% of the global population resides in areas that don't meet WHO's air quality guidelines, with 89% of these premature fatalities occurring in low or middle-income countries (WHO, 2022; Pandey et al., 2021). To address this issue, it's crucial to develop suitable sensor networks by putting the air pollution monitors or sensors at appropriate locations, meeting the requirements of various groups in the city, and providing much-needed information. Air pollutant concentrations have traditionally been monitored using reference stations (we will refer to them as monitors in this paper) which are highly accurate but also very costly, limiting their widespread deployment (Lagerspetz et al., 2019). To achieve accurate air pollution monitoring within metropolitan regions, hundreds or

even thousands of reference stations are required, which proves costly to maintain and operate (Zikova et al., 2017). However, the emergence of low-cost air quality sensors presents an opportunity for higher-density deployments and improved spatial resolution in monitoring (Spinelle et al., 2017; Castell et al., 2017). Low-cost sensors offer a cost-effective solution, reducing installation and maintenance expenses and facilitating broader spatial coverage, particularly in remote areas. Therefore, in order to balance the accuracy of monitoring along with costs involved in such instruments, we will consider deployment of both monitors and sensors in this paper.

Some studies focus on optimizing air quality monitoring networks (AQMN) using different models: physical models (Araki et al., 2015; Hao and Xie, 2018) and learning-based models (Hsieh et al., 2015). However, the accuracy of these methods relies heavily on the precision of the air quality models, and both Hao and Xie (2018) and Hsieh et al. (2015) required existing air quality measurements as inputs for their prediction models which largely depend on the quality and completeness of input data. The studies by Li et al. (2017), Brenzia et al. (2015), and Zikova et al. (2017) discuss ad-hoc placement of air quality sensors in their respective study regions or using some rules of thumb. But this shows that the placement of sensors is not optimized under the budget constraints that might be present. To address these challenges, it becomes crucial to develop more strategic approaches for placing air quality sensors. Properly optimized sensor placement can lead to a more comprehensive and accurate understanding of air pollution patterns, facilitating targeted pollution control measures and ultimately improving public health and environmental management.

Lerner et al. (2019) presents a method for optimizing sensor placement based on sensor characteristics and land use analysis. Sun et al. (2019) also proposes an optimal sensor placement strategy based on population density without relying on air pollution data. Their study highlights that humans naturally depend on the closest station to observe and obtain relevant information regarding the environment when multiple stations are present in a city. The satisfaction regarding the information increases as one moves closer to the adjacent station. Unlike Lerner et al. (2019), Sun et al. (2019) represent the benefit of placing a sensor in a particular grid to the citizens not just living in that grid but also to those living the nearby grids. However, Sun et al. (2019) has **limitations in that** it does not incorporate air pollution data as a parameter in optimization, which raises concerns about the accuracy and reliability of the obtained results. Furthermore, both Lerner et al. (2019) and Sun et al. (2019) only consider deployment of one type of sensor but as we discussed **previously**, both monitors (that are very accurate) and sensors (that are not that accurate but much more economical than monitors) should together be considered for deployment.

~~In this paper, we propose deploying a combination of low-cost sensors (referred to as sensors) and reference stations (referred to as monitors), termed hybrid instruments, in a specific region.~~ Note that Castell et al. (2017) also highlighted that sensors alone may not provide accurate air quality measurements as compared to reference instruments or monitors. Our proposed approach aims to leverage the strengths of both sensors and monitors to enhance air quality monitoring in a cost-effective manner. We propose to develop a framework for placing hybrid instruments with the objective of maximizing the public

65 satisfaction by considering emission spread and population density as parameters (while considering the benefit of placing
instruments in nearby grids ~~also~~ and not just the grids where they are placed). Also, several **notable** constraints such as having
at least one sensor in a given set of important grids (like important residential or commercial areas), not having monitors in
certain given grids (like places with sparse population, water bodies, etc.), having a minimum number of grids where monitors
should be placed in the network, etc., have been proposed in the optimization formulation. **Therefore, the following** are the
70 contributions of our work:

- Our research focuses on optimal deployment of hybrid air-quality monitoring networks consisting of monitors and sensors where the goal is to maximize public satisfaction by providing accurate air quality information while considering several budget and other constraints.
- We propose a Genetic algorithm (GA) and a greedy algorithm (GrA) to solve the developed optimization problem.
- We test the developed algorithms on networks of varying sizes and geographic locations.

75

This paper's remaining sections are organized as follows: Section 2 describes the optimization problem and presents the algorithms for solving the problem. **The nNext section** provides the numerical results tested using different algorithms under different settings. The final section concludes our study and provides future directions.

2 Methodology

80 This section is divided into two parts. The first part describes the problem statement for optimization **of a hybrid** instrument network. The second part describes the methods proposed to solve the optimization problem. The second part is further subdivided into two sub parts: GA and GrA respectively.

2.1 Problem Statement

85 **Our approach focuses on placing sensors and monitors in order to maximize a utility function quantifying popular satisfaction with the instrument sensor-placements.** Realising that humans naturally depend on the closest station to observe and obtain relevant information regarding the environment when multiple stations are present in a city, we assume that an **individual's satisfaction $g(d)$ with a sensor deployment system is a function of his or her distance d to the closest sensor or monitor ~~d~~** (Sun et al., 2019). Intuitively, the satisfaction with the information increases as one moves closer to the adjacent station. **That is because people will have higher confidence on the readings by sensors or monitors that are closer to them rather than readings from instruments that are farther from them.** Therefore, $g(d)$ must satisfy the following conditions as stated in Sun et al.
90

(2019): (i) $g(d)$ must be a ~~strictly~~-decreasing function, i.e., for any $d_1 \leq d_2$, $g(d_1) \geq g(d_2)$, (ii) for any $d \geq 0$, $g(d) \geq 0$ and $g(0) = 1$. The foremost condition corresponds to the relation of satisfaction function with distance, while the latter ones assure the fact that the $g \in [0, 1]$ and g is the highest when the distance is zero. The following exponentially decreasing function $g(d)$ readily satisfies the aforementioned conditions (Sun et al., 2019):

$$g(d) = \exp\left(-\frac{d}{\theta}\right), \quad (1)$$

where θ is an exponential decay constant¹. The exponential decay function is often chosen in similar studies and practical applications because of its simplicity and effectiveness in modelling the attenuation of signal or influence with increasing distance in studies such as Sun et al. (2019). It aligns with the intuitive idea that the influence of air quality monitoring decreases as one moves farther away from the monitor. We also present the results with another appropriate satisfaction function later.

Note that monitors and sensors are not differentiated while determining the satisfaction function in our problem. That is because in many practical air quality monitoring scenarios, users may not be either interested or be able to distinguish between data collected from monitors and sensors (if the information related to the type of instrument is not openly available). From the user's perspective, the primary concern may be just to obtain reasonable air quality information, rather than worry about the specific source of the data.

In accordance with the standard procedure for environmental monitoring (Krause et al., 2008, Hsieh et al., 2015), we divide the city into distinct, equal-sized square grids. Then, we place our hybrid instruments (sensors and monitors) in these fragmented grids. Let $V = \{a | a = 1, 2, \dots, n\}$ represent a set of grids in the interested geographical area, in which $n = |V|$ represents the total number of grids. For each $a \in \{1, 2, \dots, n\}$, let p_a represent the percentage of people living in grid a , e_a represents the percentage of $PM_{2.5}$ emissions² in grid a and m_a denotes the weighted average of p_a and e_a of grid a , i.e., $m_a = (w_1 * p_a) + (w_2 * e_a)$, where $0 \leq w_1, w_2 \leq 1$ and $w_1 + w_2 = 1$. Note that both population density and $PM_{2.5}$ emissions percentage are important factors while deciding the relative importance of various grids. Population density reflects the concentration of people residing in that grid, while the $PM_{2.5}$ emissions are an indicator of the level of fine particulate matter in the air within that grid (secondary aerosol production and pollution transport also play a role in the concentrations but they are not considered here due to lack of data). Doing a weighted average of the corresponding percentage values of these parameters provides a single value that quantifies the importance of a particular grid and allows comparing between different grids. Also, if we do not the weighted averaging, and individually minimize some metrics related to emission and population then it will result into a multi-objective optimization problem which is much more difficult to solve and analyze (Deb, 2001).

¹ Depending on the largest distances that are considered in a grid network and the precision that is being considered, θ should be appropriately decided. For instance, if the computation precision being used is say about 10^{-5} and the largest distance is say 10 units then $\theta = 1$ might be reasonable since $e^{-\frac{10}{1}} = 4.5 * 10^{-5}$.

² We acknowledge with the distinction between $PM_{2.5}$ emissions and $PM_{2.5}$ concentrations (which are to be measured by the network), with the possible impacts of secondary aerosol formation and pollution transport not being accounted for by using emissions information alone. In our approach, we initially prioritize $PM_{2.5}$ emissions as the foundational data for instrument placement. However, the placement of the instruments can be updated as better estimates of $PM_{2.5}$ concentrations become available after the initial placement of sensors.

We will now introduce some variables to define the optimization formulation. **The notations are summarized in Table 2 of appendix.** Let S be a set of grids where instruments (sensors and monitors) are placed (i.e., set S consists of ~~all~~each grids a such that at least a sensor or a monitor is placed at grid a ($z_a = 1$)). For each grid $a \in \{1, 2, \dots, n\}$, let x_a be equal to one, if a sensor is placed at grid a otherwise it is equal to zero, y_a be equal to one if a monitor is placed at grid a , otherwise it is equal to zero and z_a be equal to one if any instrument is placed at grid a , otherwise it is equal to zero. Let c be the cost of a sensor, c' be the cost of a monitor and P be the total available budget. Let B be the set of grids where at least one sensor should be placed. Let C be the set of grids **where a monitor** cannot be placed. Let h be the minimum number of monitors that should be deployed. Let M be a very large positive number and m be a very small positive number. The formulation for optimally placing hybrid instruments is as follows:

$$\text{Max } \sum_{a=1}^n m_a \cdot g(d(a)) \quad (2)$$

$$\text{s.t. } \sum_{a=1}^n (cx_a + c'y_a) \leq P \quad (3)$$

$$\sum_{a \in B} x_a \geq 1 \quad (4)$$

$$\sum_{a \in C} y_a = 0 \quad (5)$$

$$\sum_{a=1}^n y_a \geq h \quad (6)$$

$$Mz_a + m \geq x_a + y_a, \forall a = 1, 2, \dots, n \quad (7)$$

$$x_a + y_a \geq z_a, \forall a = 1, 2, \dots, n \quad (8)$$

where $d(a) = \min_{b \in V} \{z_b \cdot d(a, b) + \bar{d}(a) \cdot (1 - z_b)\}$ and $\bar{d}(a) = \max_{b \in V} d(a, b)$.

The objective is to choose a subset of grids $S \subseteq V$ that maximizes the overall satisfaction percentage under given constraints. Here, **we define $d(a, b)$ as the distance between grid a and grid b (note that when we are finding distances between two grids we mean distances between the centres of the grids)**, $d(a)$ is the minimal distance between grid a and any grid of set S (assuming that S is not an empty set, which is the case because of the constraint in Equation (4)). The condition in Equation (3) is the budget constraint which states that the total cost of all instruments cannot exceed P . The condition in Equation (4) ensures that a sensor is placed in at least one of the grids belonging to the set B . **We do not put analogous constraints such as Equation (4) for monitors as monitors cannot be place anywhere since they need where electricity availability, they are big, heavy and costly as compared to sensors.** Equation (5) ensures that no monitor is placed at any grid belonging to the set C (these grids can belong to locations like open areas, areas near waterbodies, etc.). **However**~~Note that~~, **it may not be cost-effective or practical to deploy expensive monitors in such certain areas and thus monitor deployments are restricted, but sensor deployments are not.** The condition in Equation (6) ensures that at least h ~~number of~~ monitors are deployed. Equations (7) and

145 (8) are the definitional constraints for variable z_a . That is, they ensure that for each grid a , z_a is equal to one if $x_a + y_a \geq 1$ otherwise, z_a is equal to zero.

2.2 Methods

We will now present different algorithms to solve the proposed formulation. We will first introduce Genetic Algorithm (GA).

2.2.1 Genetic Algorithm

150 A Genetic Algorithm is a metaheuristic that is inspired by the natural selection process and genetics (Deb, 2001). It mimics the principles of survival of the fittest, crossover, and mutation to iteratively search for optimal solutions. The algorithm starts by creating an initial population of potential solutions, represented as strings of individuals. Consider a string comprising of $2n$ elements (n is the total number of grids), with the first n elements is for the placement of sensors and the next n elements is for the placement of monitors. Each element in the string can take a value of either 0 or 1, where 1 indicates the presence of a sensor or monitor (depending on whether we are looking in the first n or last n elements) in the corresponding grid, and 0 indicates the absence. We now consider a modification of the above string where we remove the elements that correspond to monitors belonging to set C . The removed elements will always have value equal to zero due to the definition of set C (consequently, monitors will not be placed on the grids belonging to the C set) and thus they are separated so that the values of these elements do not change due to different processes in GA. The aforementioned modified string is used in our problem.

160 Each string encodes a set of decision variables, representing a candidate solution to the problem.

We define a fitness metric that is used to assign a relative merit (fitness) to each solution based on the corresponding objective function value and constraint violations. The fitness, $F(H)$, of any string H is calculated as follows:

$$F(H) = \begin{cases} fn & \text{if } H \text{ is a feasible sol string} \\ fn_{min} - D_1 - D_2 - D_3 & \text{otherwise} \end{cases} \quad (9)$$

$$\text{Where, } D_1 = \begin{cases} 0 & \sum_{a=1}^n (cx_a + c'y_a) \leq P \\ \sum_{a=1}^n (cx_a + c'y_a) - P & \text{Otherwise} \end{cases} \quad (10)$$

$$D_2 = \begin{cases} 0 & \sum_{a \in B} x_a \geq 1 \\ 1 & \text{Otherwise} \end{cases} \quad (11)$$

$$D_3 = \begin{cases} 0 & \sum_{a=1}^n y_a \geq h \\ h - \sum_{a=1}^n y_a & \text{Otherwise} \end{cases} \quad (12)$$

165

Here, fn is the objective function value for string H as obtained by Equation (2), fn_{min} is the minimum value of objective function values over all the feasible solution strings in a given population of strings, and D_1 , D_2 and D_3 are penalty values for

violating constraints in Equation (3), (4) and (6), respectively. Note that there is no penalty value for violating the constraint
 170 in Equation (5) as that is automatically satisfied due to the way we define our strings (recall that we removed the elements
 corresponding to the grids of set C).

In each generation (or iteration) of GA, the Roulette Wheel Selection (RWS) is used to select solutions from a population
 based on their fitness values (Deb, 2001). RWS provides a proportional selection mechanism where fitter solutions have a
 175 higher probability of being selected, but it still allows weaker solutions to have some chance of being chosen. After the
 selection procedure, crossover procedure is followed where two strings are randomly selected from the mating pool, and a
 partial interchange from both strings is done to generate two new strings. We use the two-point crossover operator where two
 distinct crossover points divide the strings into three substrings and the middle substring is exchanged between the strings
 (Deb, 2001). After crossover, mutation procedure is **carried out** where the mutation operator alters 1 to 0 or vice versa in each
 180 element of a string with probability P_m (referred to as the mutation probability). Note that mutation helps in maintaining
 diversity in the population. After applying the genetic operators, parent population and offspring population are combined,
 strings in the combined population are sorted in non-increasing order and the top half of the combined population is selected
 as the population for the next generation. This process is repeated over multiple iterations or generations until the termination
 criteria (to be specified next) is met. We now describe the termination criteria. Let the average fitness value of strings in the
 185 population of i th iteration or generation be k_i . Let N be the maximum number of iterations of GA that are allowed. Then, the
 algorithm stops at the end of the i th iteration if $\left| \frac{k_i - k_{i-1}}{k_{i-1}} \right| \leq \alpha$ (where α is a given value) or if i becomes equal to N .

2.2.2 Greedy Algorithm

The second method to solve the optimization problem from Section 2.1 is a Greedy Algorithm (GrA). A GrA iteratively comes
 190 up with a solution by making choices that are locally optimal in each iteration but it is not guaranteed to produce an optimal
 solution. In this algorithm, we first place a sensor at one of the locations from set B to satisfy Equation (4). This placement is
 done by selecting the grid with the highest m_a among the set B . Then, we find the placement location for h monitors to satisfy
 Equation (6) by ensuring that Equation (5) (which tells us about the grids where monitors can't be placed) is not violated. We
 now define grid location s^* with largest information gain as $s^* = \operatorname{argmax}_s \sum_{a=1}^n m_a (g(d'(a, K \cup s)) - g(d'(a, K)))$
 195 where K is the set of grids that have either a sensor or a monitor already placed (note that K is not an empty set because we
 have at least one grid belonging to set B that has a sensor placed) and $d'(a, K)$ represents the minimum distance between grid
 a and any grid of set K . The placement of h monitors is done by repeatedly choosing the grid location with the largest
 information gain s^* . Let $P' = P$, where P' is the budget that remains after we **subtract** the cost of different instruments that are
 placed in different iterations of GrA. After the placement of one sensor plus h monitors, the available budget $P' = P - c -$
 200 hc' . After satisfying Equation (6), there is no benefit of placing more monitors that are costly and thus we target to place

sensors. We keep placing sensors such that the grid location with the largest information gain s^* is selected while ensuring that P' is updated with every placement of sensor and budget constraint is satisfied. **The algorithm terminates when there is an insufficient budget to place sensors, i.e., when $P' < c$.**

205 We now provide an example of a 3x3 network (i.e., a network having $3 \times 3 = 9$ grids) to illustrate the greedy algorithm. The population density data and PM_{2.5} emissions data for a 3x3 network are provided below on the left and right, respectively.

<u>65646</u>	<u>29660</u>	<u>15504</u>
<u>9487</u>	<u>2984</u>	<u>2260</u>
<u>2042</u>	<u>2393</u>	<u>1711</u>

<u>0.143405</u>	<u>0.120589</u>	<u>0.097773</u>
<u>0.114025</u>	<u>0.142434</u>	<u>0.170843</u>
<u>0.084646</u>	<u>0.16428</u>	<u>0.243914</u>

Then we calculate the percentage of population density (p_a) and PM_{2.5} emissions (e_a) for each grid and then calculate m_a which is an average of p_a and e_a . The following tables show the values of p_a (left) and e_a (right).

<u>49.85</u>	<u>22.5231</u>	<u>11.7734</u>
<u>7.2042</u>	<u>2.266</u>	<u>1.7162</u>
<u>1.5506</u>	<u>1.8172</u>	<u>1.2993</u>

<u>11.1868</u>	<u>9.407</u>	<u>7.6271</u>
<u>8.895</u>	<u>11.111</u>	<u>13.3273</u>
<u>6.6031</u>	<u>12.8153</u>	<u>19.0274</u>

210

The following values are the m_a values for each grid of the 3x3 network that we consider.

<u>30.5184</u>	<u>15.965</u>	<u>9.7002</u>
<u>8.0496</u>	<u>6.6885</u>	<u>7.5217</u>
<u>4.0769</u>	<u>7.3162</u>	<u>10.1633</u>

215

Suppose the set B in which at least one sensor is to be placed from Equation (4) is consists of grids 7 and 9 and set C in which no monitor can be placed from Equation (5) is given by set 7. Suppose $h = 2$, which represents the minimum number of monitors required. Let the cost of sensor (c) and monitor (c') be 200 and 8000 units respectively. The total available budget be 16500 units.

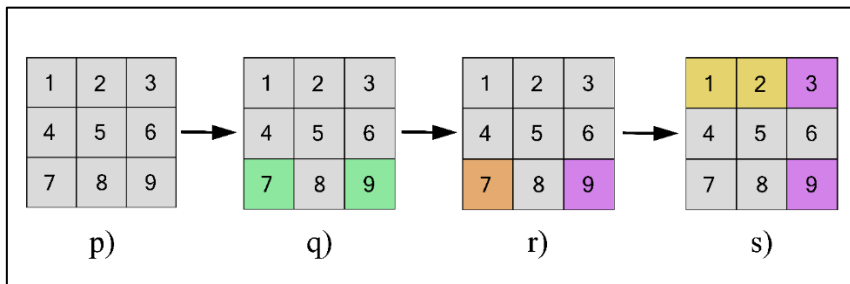


Fig. 1 Example to show the working of greedy algorithm

220

Figure 1p) shows the initial empty grids which are grey in color. Figure 1q) shows the grid area in which two grids (i.e., grids 7 and 9) are shown in light green color grids which tells us about grids in set B , where at least one sensor must be placed. Given that the value of m_a for grid 9 is greater than that of grid 7, a sensor is initially placed in grid 9 to satisfy Equation (4). The placement of a sensor at grid 9 reduces the available budget to 16300 units.

225

Figure 1r) shows the placement of sensor at grid 9 and a grid (corresponding to set C) which is shown by orange colored square grid (i.e., grid 7). The monitors are positioned at grid 1 and 2 based on the values obtained from the largest information gain s^* and in adherence to the Equation (5) which has a requirement that no monitor be placed on any grid belonging to set C . This further reduces the budget from 16300 units to 300 units by subtracting 16000 units (i.e., $c'h$)

230

We continue to place sensors until the budget constraint is violated. We will place next sensor at the grid with largest information gain s^* and that grid is grid 3. This further reduces the budget from 300 units to 100 units. The algorithm stops here as there is no sufficient budget to proceed. Figure 1s) shows the final solution using greedy algorithm where grey colored square grids show the empty grids, purple colored square grids shows the placement location of sensors and light yellow colored square grids shows the placement location of monitors.

3 Results

235

In this section, we will present results by testing our proposed algorithms in different settings. Our algorithms have been employed in two distinct areas within Surat and Mumbai cities. Both algorithms were implemented in MATLAB and executed on a computer with Intel® Core™ i7-2600 processor and 8 GB RAM.

3.1 Surat City

240

We first consider a portion of Surat which is a major city in the state of Gujarat, India, for optimal placement of air quality instruments. In this study, we take a pilot project area of 5 km x 5 km in Surat and divide it into 25 grids (thus each grid is of the size 1 km x 1 km). The total number of grids in Surat are 25 which are numbered from 1 to 25 from left to right in the increasing order and from top to bottom in the increasing order (see Figure 2). For calculating the optimal locations for hybrid instruments, we use the average percentage of population density (WorldPopBank provides open source³ population density data at a spatial resolution of 1 km x 1 km) and PM_{2.5} emission data (The Energy and Resources Institute (TERI) provides us PM_{2.5} emission data for Surat city at a spatial resolution of 1 km x 1 km) for the part of Surat city that we focus. Figures 3 and 4 provide the population density data (in population per sq. km) and emissions data (in kT/yr) for the grids for Surat City that are considered in this paper.

245

³ <https://hub.worldpop.org/geodata/summary?id=41746>

<u>1</u>	<u>2</u>	<u>3</u>	<u>4</u>	<u>5</u>
<u>6</u>	<u>7</u>	<u>8</u>	<u>9</u>	<u>10</u>
<u>11</u>	<u>12</u>	<u>13</u>	<u>14</u>	<u>15</u>
<u>16</u>	<u>17</u>	<u>18</u>	<u>19</u>	<u>20</u>
<u>21</u>	<u>22</u>	<u>23</u>	<u>24</u>	<u>25</u>

Fig 2. Numbering of grids in the portion of Surat City that are considered.

250

<u>44252</u>	<u>74524</u>	<u>85060</u>	<u>66989</u>	<u>94922</u>
<u>23631</u>	<u>50185</u>	<u>74016</u>	<u>80964</u>	<u>86887</u>
<u>40666</u>	<u>69841</u>	<u>65646</u>	<u>29660</u>	<u>15504</u>
<u>29549</u>	<u>21068</u>	<u>9487</u>	<u>2984</u>	<u>2260</u>
<u>4267</u>	<u>2293</u>	<u>2042</u>	<u>2393</u>	<u>1711</u>

Fig 3. Population density data for Surat City (in population per sq. km).

<u>0.29385</u>	<u>0.497288</u>	<u>0.700726</u>	<u>0.665802</u>	<u>0.630877</u>
<u>0.199782</u>	<u>0.310924</u>	<u>0.422065</u>	<u>0.393195</u>	<u>0.364325</u>
<u>0.105715</u>	<u>0.12456</u>	<u>0.143405</u>	<u>0.120589</u>	<u>0.097773</u>
<u>0.056277</u>	<u>0.085151</u>	<u>0.114025</u>	<u>0.142434</u>	<u>0.170843</u>
<u>0.006839</u>	<u>0.045742</u>	<u>0.084646</u>	<u>0.16428</u>	<u>0.243914</u>

Fig 4. PM2.5 emissions data for Surat City (in kT/yr).

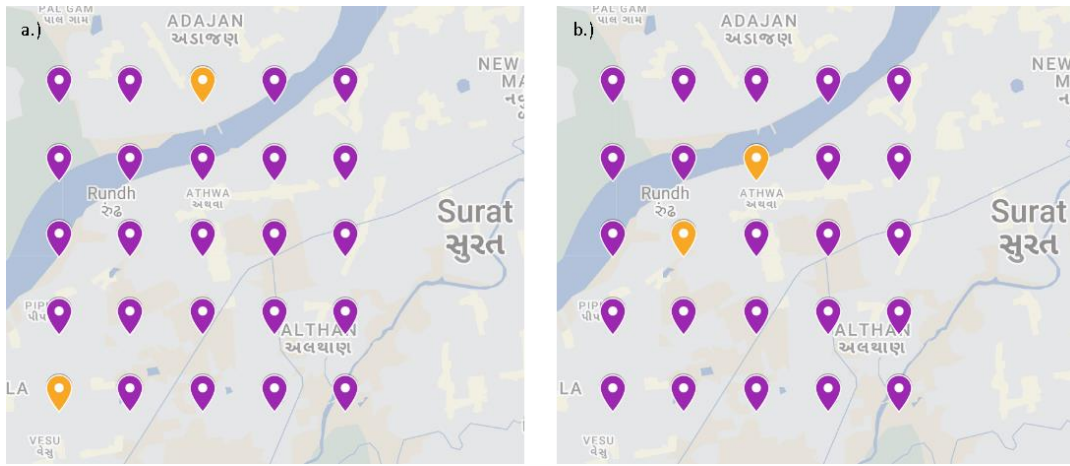


Fig 51. Hybrid ~~sensor~~ placement obtained by GA (left) and GrA (right) for the Surat network with budget value of \$313000. Map data © 2023 Google.

Figure 51 displays the placement locations of sensors (purple points) and monitors (orange points) in Surat city as obtained by Genetic algorithm (left) and Greedy algorithm (right). In Figure 51, the Greedy algorithm (GrA) places monitors close to each other due to its methodology. That is because after placing one sensor at a grid in set B , the algorithm then positions monitors at grids with the highest s^* values. This leads to monitors being placed close together, as seen at grids 8 and 12. In contrast, the solutions of the Genetic algorithm are generated through a probabilistic process and thus may exhibit a different spatial distribution than that obtained by the Greedy Algorithm. Note that the objective function value corresponding to both the algorithms for this case is equal to 100 (see Figure 6) but the spatial distribution of the instruments is not the same. That is because this is a discrete optimization problem and it can also be possible that two solutions with very different looking spatial distribution can have the same objective function value. Also, note that the weights taken for Surat city in the objective function are $w_1 = w_2 = 0.5$. That is because $PM_{2.5}$ emissions and population density are two essential factors for air quality sensor placements. By averaging these variables, we strike a balance between the need to monitor areas with high pollution levels (captured by $PM_{2.5}$ emissions) and areas with high population density (captured by the population density). Note that we will present the sensitivity analysis with different We have also taken different weights values for the sensitivity analysis later. The parameter values that are used in this placement are as follows: cost of a sensor (c) is \$3000, cost of a monitor (c') is \$122000,⁴ total available budget (P) is \$313000, value of θ and h are 1 and 2, respectively. The GA parameters that are used are as follows: population size is equal to 1000, mutation probability (P_m) is equal to 0.1, maximum

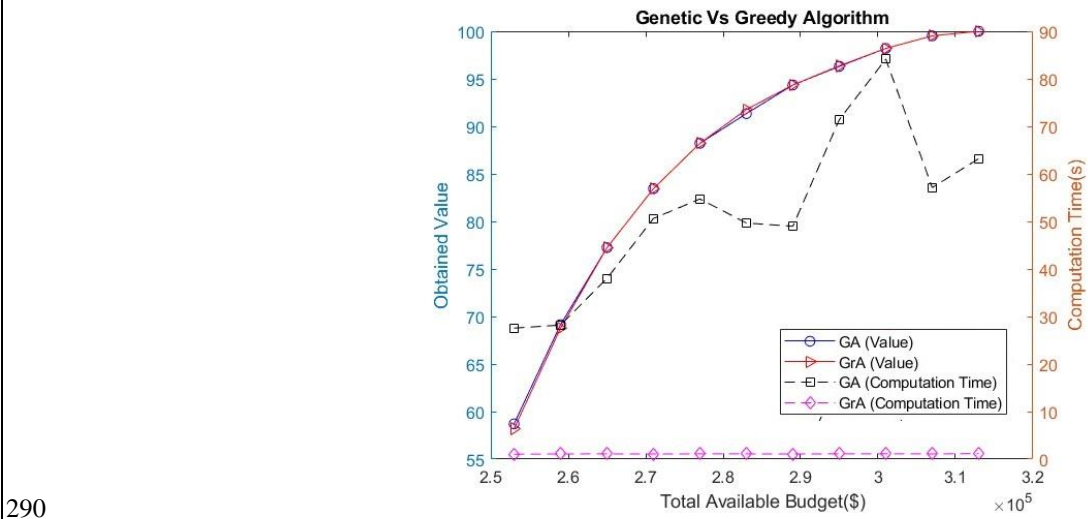
⁴ We obtained the cost estimate for a monitor through the cost of continuous ambient air quality monitoring stations (CAAQMS) imported to India whose price is available at the following link: <https://timesofindia.indiatimes.com/india/centre-asks-states-not-to-procure-imported-air-quality-monitors-indigenous-systems-to-be-deployed/articleshow/95901936.cms>. Similarly, the cost of a sensor (here Aeroqual S500) is estimated from the following link: <https://www.cleanair.com/product/aeroqual-s500-starter-kit/>.

275 number of iterations or generations is 500 and value of α is 10^{-5} . Note that we determined that $\alpha = 10^{-5}$ consistently yielded satisfactory convergence while ensuring computational efficiency through systematic tuning involving a range of α values.

Figure 62 shows the values obtained and computational time for the two algorithms, considering different total available budgets (i.e., P). Note that the obtained value on the left vertical axis in Figure 62 is objective function value which is the summation of multiplication of m_g and $g(d)$ over all grid points as given by Equation (2).

280 The minimum budget that is considered is \$253,000, which is equal to the cost of three sensors plus h monitors (any value of budget lower than this will not yield a feasible solution of the problem as the other budget constraints will not get satisfied). The maximum budget in Figure 62 is \$313,000, which allows for the placement of 2 monitors and 23 sensors, covering the entire portion area (as there are a total of 25 grids) under minimum possible budget as at least 2 monitors need to be placed by

285 Equation (6). If we keep on increasing the budget, then it might be possible that the number of monitors become greater than is two increased from 2 to 3 and so on (but that would not yield any increase in the objective function value as the satisfaction function is assumed to be identical for sensors and monitors). Obtained value on the left axis in Figure 2 is objective function value which is the summation of multiplication of m_g and $g(d)$ over all grid points.



290 **Fig 62. Plot comparing genetic vs greedy algorithms for varying total available budget values.**

From Figure 62, it can be observed that, for most budget points, the obtained values for GrA and GA are very close. Also, note that the obtained values for both the algorithms increase with the increase in budget because it is possible to place more instruments with the increase in budget and that results in increase in the overall satisfaction function value. Note that the computation time of GA is significantly larger than that of GrA because GA samples through a set of possible solutions and

iteratively applies various operators such as selection, crossover and mutation whereas GrA is a deterministic algorithm that comes up with a single solution.

300

We now include an example to show the performance of different network configurations that have different variations with respect to the optimal solution. Consider an example of 3 x 3 network. Let the cost of a sensor (c) and a monitor (c') be \$3000 and \$122000 respectively. Suppose the budget value is equal to \$253000. The numbering of the grids follows the convention that numbers first increase as we go from left to right in the increasing order and numbers increase as we go from top to bottom.

305

Let the set B in which at least one sensor is to be placed from Equation (4) consist of grids 7 and 9 and set C in which no monitor can be placed from Equation (5) be set 7. We consider four different feasible solutions as follows:

Case 1: Solution obtained from greedy algorithm.

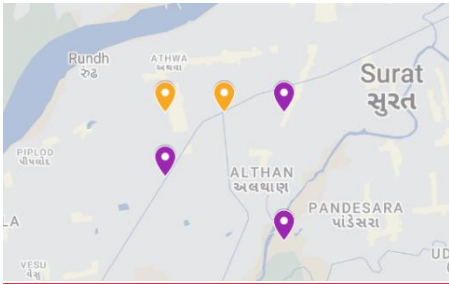


Fig 7. Hybrid placement obtained by GrA.

310

Figure 7 shows the solution that is obtained in Case 1. The purple points show the placement location of sensors and orange points show the placement location of monitors. It can be seen that monitors are placed at grids 1 and 2 and sensors are placed at grids 3, 4 and 9.

Case 2: Sensor placed at grid 3 in Case 1 is moved to grid 7 (all the other instrument locations remain the same as in Case 1).

315

Case 3: Monitor placed at grid 1 in Case 1 is moved to grid 5 (all the other instrument locations remain the same as in Case 1).

Case 4: When sensor placed at grid 3 in Case 1 is moved to grid 7 and monitor placed at grid 1 in Case 1 is moved to grid 5 (all the other instrument locations remain the same as in Case 1).

The following table shows the values that are obtained for different cases.

<u>Case</u>	<u>Obtained Value</u>
<u>Case 1</u>	<u>83.8154</u>
<u>Case 2</u>	<u>80.2608</u>
<u>Case 3</u>	<u>68.7521</u>
<u>Case 4</u>	<u>65.1975</u>

320

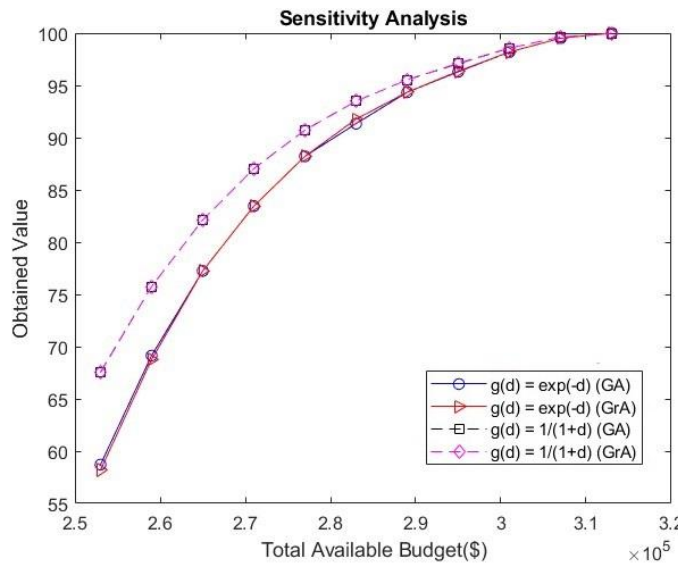
It can be seen that Case 1 has the largest value and the value decreases as we go from Case 1 to Case 4. Thus, Case 1 is the closest to the optimal solution and Case 4 is the farthest. Note that Case 4 has both the modifications that are made in Cases 2 and 3 with respect to Case 1. Since there was a decrease in the value as we go from Case 1 to Case 2 and a decrease in value from Case 1 to Case 3, the largest decrease in value is seen as we go from Case 1 to Case 4.

325 **3.1.1 Sensitivity Analysis**

In this section, we will present the results of sensitivity analysis for with a different $g(d)$ function and for consider different weighstage case corresponding to p_a and e_a in the objective function of m_a .

3.1.1.1 Sensitivity Analysis Results for Different $g(d) = \frac{1}{d+1}$ Function

330 As previously mentioned, the $g(d)$ function should be strictly a decreasing function. Therefore, we explore an alternative function $g(d) = \frac{1}{d+1}$, apart from the exponential function, which is $g(d) = \frac{1}{d+1}$, referred to as the "new function.". We have now obtained the results by greedy algorithm and genetic algorithm for Surat city grid network (5x5 size) using $g(d) = \frac{1}{d+1}$, while keeping all the other parameters the same (as in Figure 6).



335 **Fig. 83. Plot comparing different two functional forms of $g(d)$ by using genetic & greedy algorithms for varying total available budget values.**

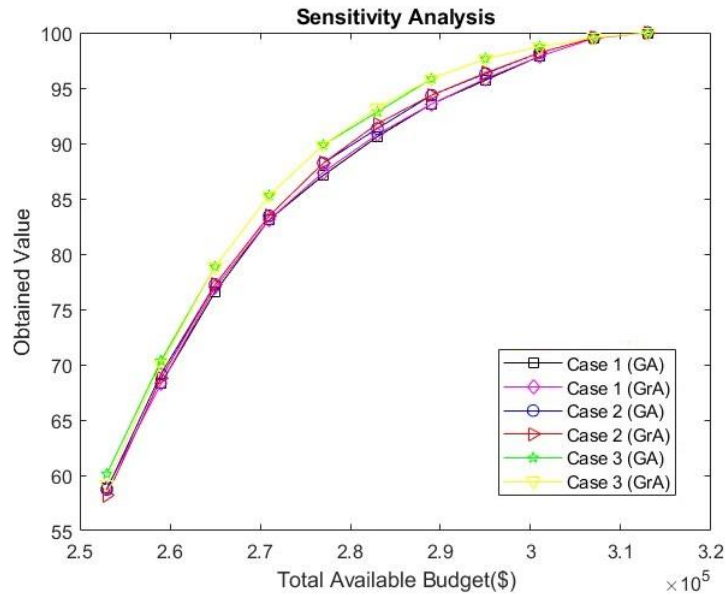
340 Figure 8 presents the values obtained by different algorithms and functional form for $g(d)$ with varying budget values. It can be seen in the above figure that the values obtained by the genetic algorithm and the greedy algorithm for $g(d) = e^{-d}$ are very close and thus the solid blue and red curves almost overlap. The same holds for $g(d) = \frac{1}{d+1}$ and therefore the dashed black and purple lines almost overlap. Note that the values that are obtained by the two algorithms for $g(d) = \frac{1}{d+1}$ are greater than that obtained for $g(d) = e^{-d}$. That is because $\frac{1}{d+1} > e^{-d}$ for all positive values of d . However, notice that the pattern of the values that are obtained for the two functional forms is the same, i.e., the values decrease as the total available budget increases. Also, notice that the values obtained by the two functional forms converge at the budget value of \$313,000. Since it is not possible to have percentage values greater than 100, the values for both the functional forms will remain the same for budget values greater than \$313,000. We believe that similar patterns will be observed by other functional forms of $g(d)$ as long as they satisfy the conditions that are necessary for satisfaction functions (i.e., $g(d)$ must be a decreasing function and $g(0) = 1$).

350 **3.1.1.2 Sensitivity Analysis for different Different-Weightage in the objective function Cases**

We have also conducted the sensitivity analysis by varying the weightage between the percentages of pPopulation density and PM2.5 emissions (i.e., p_a and e_a) for Surat city of 5 km x 5 km area. Table 1 shows the weights corresponding to the different cases that have been considered. We have determined the results for both Greedy algorithm and Genetic algorithm is used for this sensitivity analysis by keeping all the parameters same (as in Figure 6).

Table 1. It shows values taken for different cases for the weightage of population density and PM2.5 emissions weights

Case	Weightage of Population Density for p_a	Weightage of PM _{2.5} emissions for e_a
1	0.25	0.75
2	0.5	0.5
3	0.75	0.25



360 **Fig. 94. Plot comparing the three cases for different weights corresponding to p_a and $e_a \cdot m_a$ by using genetic & greedy algorithms for varying total available budget values.**

365 Figure 9 shows the values that are obtained for different cases, budget values and algorithms. As before, the values obtained by GA and GrA are very close for given weights and budget. Among these cases, the values corresponding to Case 3 (where $p_a = 0.75$ and $e_a = 0.25$) are the highest and that corresponding to Case 1 (where $p_a = 0.25$ and $e_a = 0.75$) are the lowest. Thus, as the relative weightage for population density increases in the objective function, the values obtained increases. However, it can be seen that the difference between the values for Cases 1 and 3 is not that large, signifying that the objective function values may not be that sensitive to the relative weightage between population density and emissions.

370 3.2 Mumbai City

We now present the results that we tested for portions of Mumbai, which is the financial hub of India. In this case, we only considered the contribution of population in the objective function (i.e., $w_1 = 1$, & $w_2 = 0$, implying which means $m_a = p_a$) due to unavailability of $PM_{2.5}$ emission data for Mumbai city. However, the aforementioned change does not have any significant issue on the results that we present as we plan to test the effect of varying the budget (as in the last section) and the effect of varying the size of the network (i.e., the number of grids). All the parameter values for the algorithm's execution were the same as in the example for Surat city (i.e., Figure 6), except for the variable θ , which has now been set to 5 (note that θ has been increased now because we have a larger a-number of grids in Mumbai network as compared to Surat, resulting in higher

average distances between the grids for the Mumbai network and thus we need to update θ for better normalization). Consider a region of size 10 km x 10 km in Mumbai City that has been divided into 100 grids (i.e., each grid is of the size 1 km x 1 km). Figure 105 shows the variation of values obtained and computation time with total available budget for GA and GrA for this region. The solid lines represent the obtained values and dashed lines are used to represent the computation time in seconds for different algorithms. It can be seen that the genetic algorithm (GA) provides higher value as compared to the greedy algorithm (GrA) for most of the cases. Thus, it highlights the importance of GA in obtaining values that are closer to the optimal as compared to GrA when the network size increased (however this advantage comes at the high computational cost of GA as compared to GrA).

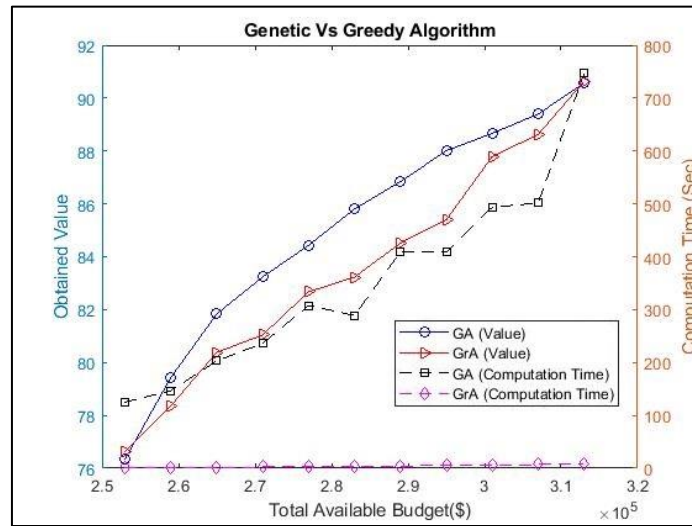
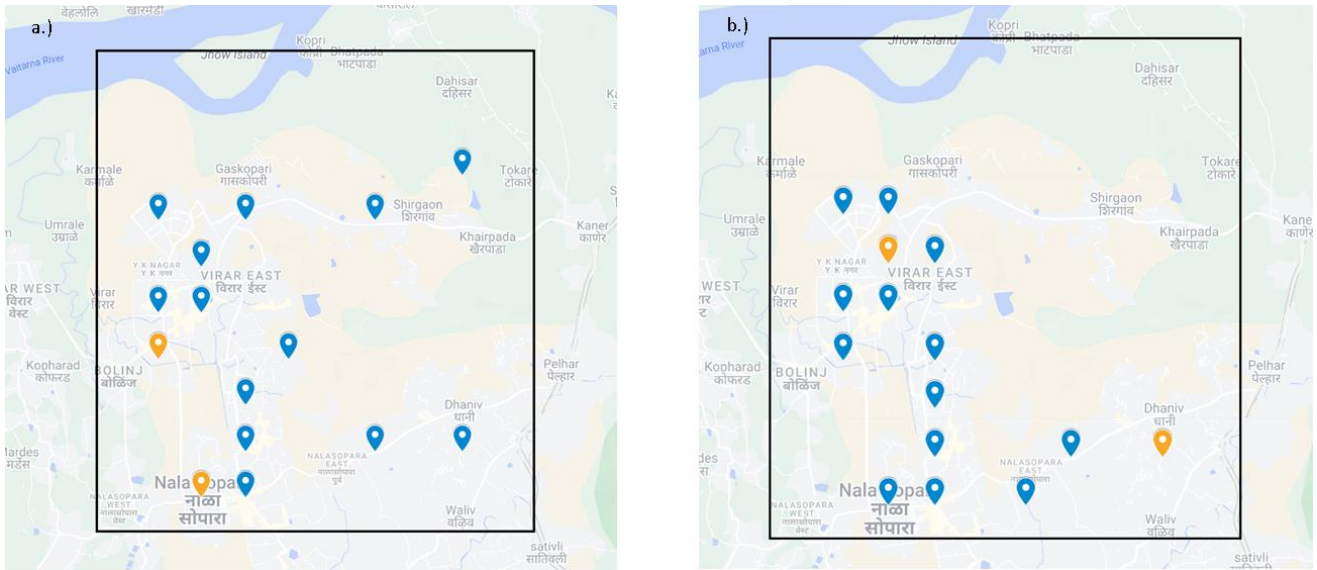


Fig 105. Plot comparing genetic versus greedy algorithm for varying total available budget values.

Figure 116 shows ~~us~~ the placement of hybrid instruments obtained for the two algorithms (GA and GrA) when the budget is equal to \$283000 when we have all the parameters the same as that in Figure 105. The blue and orange points represent the placement of sensors and monitors, respectively. In Figure 116a, two sensors are positioned in the northeast area, while no sensors or monitors are placed in that area in Figure 11bGrA. In Figure 11bGrA, monitors/sensors are predominantly concentrated on the left side of the Mumbai area, whereas in Figure 11aGA, the sensors/monitors exhibit a more diverse and scattered distribution. Note that out of 100 grids, sensors and monitors can be placed in only 15 grids by maximizing the objective function. The leftmost and southern areas have the highest population density, which explains the concentration of sensors and monitors in those regions. From Figure 6b that represents the hybrid sensor placement by GrA, it is evident that sensors and monitors are mainly concentrated in the bottom leftmost region. In contrast, Figure 6a shows a more diverse or scattered distribution of sensors and monitors. There is difference in the solutions that are obtained by the two algorithms. It is

400 because GA samples through various solutions that to proceed towards a solution is closer to the optimal whereas GrA is a deterministic algorithm and may get stuck near a locally optimal solution.



405 **Fig 116.** Sensor placement obtained by GA (left) and GrA (right) for 10 km x 10 km (100 grids) region in Mumbai when the budget is equal to \$283000. Map data © 2023 Google.

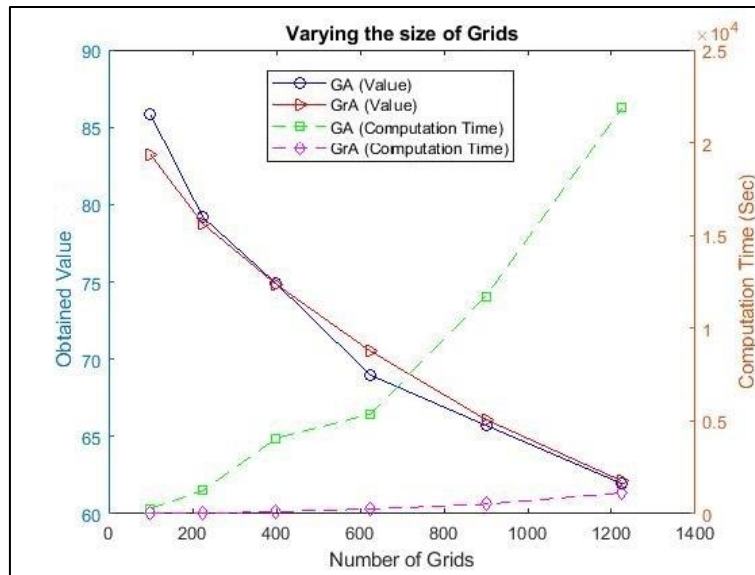


Fig 127. Plot comparing genetic and greedy algorithms for varying number of grids.

In Figure 6, two sensors are positioned in the northeast area, while no sensors or monitors are placed in that area in GrA. In GrA, monitors/sensors are predominantly concentrated on the left side of the Mumbai area, whereas in GA, the sensors/monitors exhibit a more diverse and scattered distribution. Note that out of 100 grids, sensors and monitors can be placed in only 15 grids by maximizing the objective function. The leftmost and southern areas have the highest population density, which explains the concentration of sensors and monitors in those regions. Figure 127 shows the comparison between GA and GrA with varying number of grids for the budget value of \$283000.⁵ The solid lines represent the obtained values in percentage for different algorithms and dashed lines are used to represent the computation time in seconds for different algorithms. As the number of grids increases, there is a noticeable decline in citizen satisfaction (i.e., the obtained values) because the budget P remains the same and thus the satisfaction averaged across all the grids reduces as it gets distributed across the total region (note that the percentage of population in each grid also reduces as the number of grids increase and thus that also contributed to the observed trend). Also, the values obtained by GA and GrA are similar and in some cases GA outperforms GrA whereas the reverse happens in other cases. Note that the computation time required for GA increases rapidly with the increase in the number of grids because with the increase in the number of grids, the size of each string in GA increases and it takes more iterations before the termination criterion is reached in GA (as the number of feasible solutions increase with the increase in grid size). However, the increase in the computational time of GrA is not that high as it is a polynomial-time algorithm (Cormen et al., 2022), i.e., the computational time increases polynomially with respect to the increase in the problem size (i.e., the number of grids in our problem).

4 Conclusions

This research paper proposed an optimization formulation for placement of hybrid instruments (sensors and monitors). The objective of the problem is to maximize the satisfaction function while satisfying various constraints for the placement. To solve this formulation, we proposed two algorithms: a genetic algorithm (GA) which is a metaheuristic that works using the principles of evolution and a greedy algorithm (GrA) that makes choices that are locally optimal in each iteration. We tested the placement solutions generated by these algorithms on networks from different locations (Surat and Mumbai) that differed over sizes and characteristics (population distribution, budget and $PM_{2.5}$ distribution). We observed that as the total available budget increased, the obtained values from the two algorithms also increased as it became possible to place more instruments (sensors and monitors). We found that GrA is very computationally efficient as compared to GA, but we found that both GrA and GA provided close values (in some cases GA outperformed GrA whereas in other cases the reverse happened). Note that since GA searches through a set of solutions over multiple iterations and uses operators like mutation it has a better likelihood of getting towards the optimal solutions whereas GrA may get stuck near a local optimum in some cases. These findings

⁵ The population data (in terms of population per square km) is available at the following link: https://docs.google.com/spreadsheets/d/1tdDUXnu4EQb2t3g_M96RXb4mkRXdaFP3/edit#gid=1468141414. This data contains the largest set of grids used with $35 \times 35 = 1225$ grids. There are two sheets, one shows the numbering of grids and the other contains the population data. The population data for both Surat and Mumbai have been obtained from the following website: <https://hub.worldpop.org/geodata/summary?id=41746>

440 suggest that if time is not constrained (i.e., we have a few days to decide the placement solution) it might be better to use GA
and GrA together (i.e., use the best solution out of the two algorithms) to place the instruments whereas in scenarios where
there is scarcity of time, it is advised to use GrA. While the study's results are specific to these locations, the underlying
methodology and principles learned from these cases can be broadly applied to other areas facing similar air quality monitoring
challenges. The methodology presented in our paper serves as a template for optimizing sensor networks in any location,
445 provided that relevant data on population, emissions, and potential grid locations are available. Our research aims to provide
valuable insights for future government decision-making processes regarding the optimal deployment of hybrid instruments
in cities lacking an existing sensor network.

~~T~~But there are several interesting future extensions of this work that are possible. We acknowledge the challenges associated
450 with quantifying PM_{2.5} emissions in areas lacking an established monitoring network, as evident in the Mumbai case.
However, in future, solutions such as considering existing models or satellite-derived data as proxies for local PM_{2.5}
concentrations during the network design phase can be implemented. Also, after the placement of instruments, one could
iteratively update the placement of the network using some existing models or proxy data as newly collected data update the
prior estimates of concentrations in the different grid cells. In addition, we assumed a particular form of the satisfaction function
455 (consisting of exponential terms) but other forms can also be tested. Similarly, other factors apart from population density and
PM_{2.5} concentrations such as socio-economic disparities across various grids can also be factored while determining the
satisfaction function. Note that exploring other objective functions such as improving estimates of population exposure,
monitoring the largest known sources, etc., would also be very interesting. To address these alternative objectives, we could
make the following modifications to our approach. First, the objective function could be defined appropriately whether it is
460 optimizing public satisfaction, estimating exposure, or addressing specific environmental issues. Also, depending on the
chosen objective, we may need to adapt the data collection methods used. For example, if the goal is to estimate population
exposure, we may need to tailor the data collection frequency accordingly. The analysis methods and models used for decision-
making can be customized based on the objective. For instance, if the goal is to address specific environmental concerns,
sophisticated modelling techniques may be employed to assess pollutant dispersion. When other objective functions are used
465 then the fitness function in the genetic algorithm will get modified. The selection, crossover and mutation operators will not
change if the constraints remain the same and there would only be change in the objective function. Similarly, the greedy
algorithm will have a modified gain function s^* and the rest of the algorithm will remain the same provided the constraints in
the problem remain the same. Thus, our approach can be flexibly adapted to address a range of objectives. Note that there is
also ~~mention the~~ potential for creating user-friendly software tools or decision support systems based on the methodology
470 presented in our paper. Such tools would enable users with limited algorithmic expertise to apply similar optimization
techniques to their specific locations, addressing the concern of not having the ability to run the algorithm. In these software
tools, the users will only have to provide input values for the problem like the network they want to solve, costs of instruments,
budget, the algorithm they want to use, etc., and the toolbox will provide the results.

Appendix

475 Table 2

Notations	Description
V	Set of all grids
n	Total number of grids
S	Set of grids selected for deploying hybrid instruments
$g(d)$	An individual's satisfaction as a function of his or her distance d to the closest sensor or monitor A function of his or her distance to the closest sensor d
θ	Exponential decay parameter
p_a	Percentage of population living in grid a
e_a	Percentage of concentration of PM _{2.5} in grid a
m_a	<u>Weighted aAverage</u> of p_a and e_a
c	Cost of each sensor
c'	Cost of each monitor
P	Total available budget
h	Minimum number of monitors to be deployed
z_a	Binary variable signifying whether a sensor or a monitor is placed at grid a or not
x_a	Binary variable signifying whether a sensor is placed at grid a or not
y_a	Binary variable signifying whether a monitor is placed at grid a or not
B	Set of grids where at least one sensor is to be placed
C	Set of grids where monitors cannot be placed
M	A very large positive number
m	A very small positive number
P_m	Mutation probability
N	Maximum number of iterations of GA that are allowed
$d(a)$	Minimum distance between grid a and the grids containing hybrid instruments
$d(a, b)$	Distance between grid a and grid b
$\bar{d}(a)$	Maximum distance between grid a and any other grid of set V
$d'(a, K)$	Minimum distance between grid a and set K

Author Contribution

HG and SNT led the conceptualization of this work. NA did the data curation. HG proposed the methodology. NA performed the coding and software part. HG and SNT supervised this work. NA prepared the original draft. All the authors contributed to review and editing.

480 Competing Interests

The contact author has declared that none of the authors has any competing interests.

Data availability

~~The data sets used in this study have been provided in the manuscript. Population Density :-~~
~~<https://hub.worldpop.org/geodata/summary?id=41746>~~

485 PM2.5 Emissions :-

~~<https://docs.google.com/spreadsheets/d/1H2enyyV7-okX13ZvCz2BiZq5ETMCAS54/edit?usp=sharing&ouid=101431267408001181537&rtfpof=true&sd=true>~~

Acknowledgements

The authors would also like to acknowledge the support of Centre of Excellence (ATMAN) approved by the office of the
490 Principal Scientific Officer to the Government of India. The CoE is supported by philanthropies including Bloomberg
Philanthropies, the Open Philanthropy and the Clean Air Fund and author SNT also acknowledges J C Bose award
(JCB/2020/000044).

References

- 495 Araki, S., Iwahashi, K., Shimadera, H., Yamamoto, K., and Kondo, A.: Optimization of air monitoring networks using chemical
transport model and search algorithm, *Atmos. Environ.*, 122, 22–30, <https://doi.org/10.1016/j.atmosenv.2015.09.030>, 2015.
- Brienza, S., Galli, A., Anastasi, G., and Bruschi, P.: A Low-Cost Sensing System for Cooperative Air Quality Monitoring in
Urban Areas, *Sensors*, 15, 12242–12259, <https://doi.org/10.3390/s150612242>, 2015.
- 500 Castell, N., Dauge, F. R., Schneider, P., Vogt, M., Lerner, U., Fishbain, B., Broday, D., and Bartonova, A.: Can commercial
low-cost sensor platforms contribute to air quality monitoring and exposure estimates?, *Environ. Int.*, 99, 293–302,
<https://doi.org/10.1016/j.envint.2016.12.007>, 2017.

- Cormen, T. H., Leiserson, C. E., Rivest, R. L., & Stein, C.: Introduction to algorithms, MIT press, ISBN 9780262046305, 2022.
- 505 Deb, K.: Multi-Objective Optimization using Evolutionary Algorithms, John Wiley, ISBN 9780471873396, 2001.
- Fuller, R., Landrigan, P. J., Balakrishnan, K., Bathan, G., Bose-O'Reilly, S., Brauer, M., Caravanos, J., Chiles, T., Cohen, A., Corra, L., Cropper, M., Ferraro, G., Hanna, J., Hanrahan, D., Hu, H., Hunter, D., Janata, G., Kupka, R., Lanphear, B., Lichtveld, M., Martin, K., Mustapha, A., Sanchez-Triana, E., Sandilya, K., Schaeffli, L., Shaw, J., Seddon, J., Suk, W., Téllez-Rojo, M. M., and Yan, C.: Pollution and health: a progress update, *Lancet Planet. Health*, 6, e535–e547, [https://doi.org/10.1016/S2542-5196\(22\)00090-0](https://doi.org/10.1016/S2542-5196(22)00090-0), 2022.
- 510 Hao, Y. and Xie, S.: Optimal redistribution of an urban air quality monitoring network using atmospheric dispersion model and genetic algorithm, *Atmos. Environ.*, 177, 222–233, <https://doi.org/10.1016/j.atmosenv.2018.01.011>, 2018.
- Hsieh, H.-P., Lin, S.-D., and Zheng, Y.: Inferring Air Quality for Station Location Recommendation Based on Urban Big Data, in: Proceedings of the 21th ACM SIGKDD International Conference on Knowledge Discovery and Data Mining, New York, NY, USA, 437–446, <https://doi.org/10.1145/2783258.2783344>, 2015.
- 515 Krause, A., Singh, A., and Guestrin, C.: Near-Optimal Sensor Placements in Gaussian Processes: Theory, Efficient Algorithms and Empirical Studies, *J. Mach. Learn. Res.*, 9, 235–284, 2008.
- Lagerspetz, E., Motlagh, N. H., Arbayani Zaidan, M., Fung, P. L., Mineraud, J., Varjonen, S., Siekkinen, M., Nurmi, P., Matsumi, Y., Tarkoma, S., and Hussein, T.: MegaSense: Feasibility of Low-Cost Sensors for Pollution Hot-spot Detection, in: 2019 IEEE 17th International Conference on Industrial Informatics (INDIN), 2019 IEEE 17th International Conference on Industrial Informatics (INDIN), 1083–1090, <https://doi.org/10.1109/INDIN41052.2019.8971963>, 2019.
- 520 Lerner, U., Hirshfeld, O., & Fishbasin, B. : Optimal deployment of a heterogeneous air quality sensor network, *J. Environ. Inform.*, 34(2), 99-107, doi:10.3808/jei.201800399, 2019.
- 525 Li, X., Ma, Y., Wang, Y., Liu, N., and Hong, Y.: Temporal and spatial analyses of particulate matter (PM10 and PM2.5) and its relationship with meteorological parameters over an urban city in northeast China, *Atmospheric Res.*, 198, 185–193, <https://doi.org/10.1016/j.atmosres.2017.08.023>, 2017.
- Pandey, A., Brauer, M., Cropper, M. L., Balakrishnan, K., Mathur, P., Dey, S., Turkgulu, B., Kumar, G. A., Khare, M., Beig, G., Gupta, T., Krishnankutty, R. P., Causey, K., Cohen, A. J., Bhargava, S., Aggarwal, A. N., Agrawal, A., Awasthi, S., Bennitt, F., Bhagwat, S., Bhanumati, P., Burkart, K., Chakma, J. K., Chiles, T. C., Chowdhury, S., Christopher, D. J., Dey, S., Fisher, S., Fraumeni, B., Fuller, R., Ghoshal, A. G., Golechha, M. J., Gupta, P. C., Gupta, R., Gupta, R., Gupta, S., Guttikunda, S., Hanrahan, D., Harikrishnan, S., Jeemon, P., Joshi, T. K., Kant, R., Kant, S., Kaur, T., Koul, P. A., Kumar, P., Kumar, R., Larson, S. L., Lodha, R., Madhipatla, K. K., Mahesh, P. A., Malhotra, R., Managi, S., Martin, K., Mathai, M., Mathew, J. L., Mehrotra, R., Mohan, B. V. M., Mohan, V., Mukhopadhyay, S., Mutreja, P., Naik, N., Nair, S., Pandian, J. D., Pant, P., Perianayagam, A., Prabhakaran, D., Prabhakaran, P., Rath, G. K., Ravi, S., Roy, A., Sabde, Y. D., Salvi, S., Sambandam, S., Sharma, B., Sharma, M., Sharma, S., Sharma, R. S., Shrivastava, A., Singh, S., Singh, V., Smith, R., Stanaway, J. D., Taghian, G., Tandon, N., Thakur, J. S., Thomas, N. J., Toteja, G. S., Varghese, C. M., Venkataraman, C., Venugopal, K. N., Walker, K. D., Watson, A. Y., Wozniak, S., Xavier, D., Yadama, G. N., Yadav, G., Shukla, D. K., Bekedam, H. J., et al.: Health and economic impact of air pollution in the states of India: the Global Burden of Disease Study 2019, *Lancet Planet. Health*, 5, e25–e38, [https://doi.org/10.1016/S2542-5196\(20\)30298-9](https://doi.org/10.1016/S2542-5196(20)30298-9), 2021.
- 530
535
540

Spinelle, L., Gerboles, M., Villani, M. G., Aleixandre, M., and Bonavitacola, F.: Field calibration of a cluster of low-cost commercially available sensors for air quality monitoring. Part B: NO, CO and CO₂, *Sens. Actuators B Chem.*, 238, 706–715, <https://doi.org/10.1016/j.snb.2016.07.036>, 2017.

545 Sun, C., Li, V. O. K., Lam, J. C. K., and Leslie, I.: Optimal Citizen-Centric Sensor Placement for Air Quality Monitoring: A Case Study of City of Cambridge, the United Kingdom, *IEEE Access*, 7, 47390–47400, <https://doi.org/10.1109/ACCESS.2019.2909111>, 2019.

WHO, Ambient (outdoor) air pollution: [https://www.who.int/news-room/fact-sheets/detail/ambient-\(outdoor\)-air-quality-and-health](https://www.who.int/news-room/fact-sheets/detail/ambient-(outdoor)-air-quality-and-health), last access: 19 December 2022.

550 Zikova, N., Masiol, M., Chalupa, D. C., Rich, D. Q., Ferro, A. R., and Hopke, P. K.: Estimating Hourly Concentrations of PM_{2.5} across a Metropolitan Area Using Low-Cost Particle Monitors, *Sensors*, 17, 1922, <https://doi.org/10.3390/s17081922>, 2017.